Effect of Battery Degradation on Multi-Service Portfolios of Energy Storage

Aramis Perez, Rodrigo Moreno, *Member, IEEE*, Roberto Moreira, *Member, IEEE*, Marcos E. Orchard, and Goran Strbac, *Member, IEEE*

***Abstract*—In an electricity market environment, energy storage plant owners are remunerated for the provision of services to multiple electricity sectors. Some of these services, however, may accelerate battery aging and degradation and hence this needs to be properly balanced against associated services remunerations. In this framework, we propose a combined economic-degradation model to quantify effects of operational policies (mainly focused on constraining State of Charge –SOC– to prescribed levels in order to reduce effects of aging) on gross revenue, multi-service portfolios, degradation and lifespan of distributed energy storage plants that can provide multiple services to energy and balancing market participants and Distribution Network Operators (DNO). Through various case studies based on the Great Britain (GB) system, we demonstrate that although operational policies focused on battery damage reduction will lead to a revenue loss in the short-term, such loss can be more than compensated by long-term revenues due to a lengthier battery lifespan. We also demonstrate that operational policies to reduce battery degradation mainly affect services related to the energy (rather than balancing) market, which represents a smaller proportion of the overall revenue streams of a distributed storage plant. The model is also used to study effects of ambient temperature fluctuations.**

***Index Terms*—Distributed energy storage, multi-service portfolios, degradation, temperature control, power system economics.**

I. Nomenclature

A. Parameters

$\overline{C}^S$	Storage maximum charging capacity	[MW]
$\overline{D}^S$	Storage maximum discharging capacity	[MW]
$\overline{E}$	Storage maximum energy capacity	[MWh]
P_t^D	Active power demand from distribution network at period *t*	[MW]
Q_t^D	Reactive power demand from distribution network at period *t*	[MVAr]
M	Auxiliary large number used for endogenous constraints relaxation (Big M)	
$\overline{S}^N$	Secured apparent power capacity of primary substation (N-1 limit)	[MVA]
$\overline{S}^S$	Storage maximum apparent power capacity	[MVA]
α, β	Robustness parameters to ensure deliverability of balancing services	[p.u.]
η	Storage roundtrip efficiency	[p.u.]
π_t^E	Energy price at period *t*	[£/MWh]
$\pi_t^{Dw.Rese}$	Availability price for downwards reserve at period *t*	[£/MW/h]
$\pi_t^{Dw.Resp}$	Availability price for downwards frequency response at period *t*	[£/MW/h]
$\pi_t^{Up.Rese}$	Availability price for upwards reserve at period *t*	[£/MW/h]
$\pi_t^{Up.Resp}$	Availability price for upwards frequency response at period *t*	[£/MW/h]
τ^{Rese}	Reserve maximum utilization time	[h]
τ^{Resp}	Frequency response maximum utilization time	[h]

B. Variables

C_t^S	Storage charging output at period *t*	[MW]
D_t^S	Storage discharging output at period *t*	[MW]
E_t	Storage energy at period *t*	[MWh]
P_t^N	Active power through primary substation at period *t* (positive refers to discharge and negative refers to charge)	[MW]
P_t^S	Storage scheduled active power output at period *t*	[MW]
Q_t^N	Reactive power through primary substation at period *t*	[MVAr]
Q_t^S	Storage scheduled reactive power output at period *t*	[MVAr]
$Rese_t^{Dw}$	Downwards reserve commitment at period *t*	[MW]
$Rese_t^{Up}$	Upwards reserve commitment at period *t*	[MW]
$Resp_t^{Dw}$	Downwards frequency response commitment at period *t*	[MW]
$Resp_t^{Up}$	Upwards frequency response commitment at period *t*	[MW]
$X_t^{Dw.Rese}$	Storage commitment status for downwards reserve at period *t*: 1 if committed, 0 otherwise	
$X_t^{Up.Rese}$	Storage commitment status for upwards reserve at period *t*: 1 if committed, 0 otherwise	

The authors are grateful for the support obtained through the "Whole Systems Energy Modelling" and "Energy Storage for Low Carbon Grids" projects funded by the UK Research Council, and "Smarter Network Storage" project funded by the UK Power Networks. In addition, Dr. Moreno and Orchard gratefully acknowledge the financial support of Conicyt-Chile (through grants Fondecyt/Iniciacion/11130612, Fondecyt/1140774, Fondap/15110019, the Complex Engineering Systems Institute [ICM:P-05-004-F, Conicyt:FBO16] and the Advanced Center for Electrical and Electronic Engineering [FB0008]). The work of Mr. Perez was supported by the University of Costa Rica (Grant for Doctoral Studies) and Conicyt-Pcha/DoctoradoNacional/2015-21150121.

A. Perez, R. Moreno, and M. Orchard are with the Department of Electrical Engineering (Energy Center) at University of Chile. R. Moreno is also with the Department of Electrical and Electronic Engineering at Imperial College London (corresponding author: rmorenovieyra@ing.uchile.cl).

R Moreira and G. Strbac are with the Department of Electrical and Electronic Engineering at Imperial College London.

C. Sets

A	Set of credible utilization levels of balancing services
T	Set of operating periods

II. Introduction

Energy storage has the potential to provide multiple services to several sectors in electricity industry and hence support activities related to generation, network and system operation. In an electricity market environment, a service provided by storage plant presents both (i) a short-term revenue or remuneration associated with its provision to a market participant (who pays for it) and (ii) a consequent long-term cost associated with its effects on capacity degradation. Capacity degradation is related to the progressive reduction in the amount of energy that can be delivered by the energy storage plant or the growth of its internal impedance, which is a function of the elapsed time since the manufacture date, as well as the usage over consecutive charge and discharge actions. Therefore, storage owners need to take a decision between constraining operation of energy storage plant to prescribed charge/discharge volumes in order to maintain battery lifespan at higher levels, or maximize short-term revenues regardless of effects of degradation in the long-term (which may drive higher cost of investment since replacement of battery equipment may become more frequent). Clearly, this decision will have important effects on the portfolio of services provided by energy storage plant.

Various studies have investigated the ability of energy storage plants to support integration of low carbon generation [1,2], provide balancing services [3], support energy market operations [4,5], and alleviate network congestion [6]. Recent studies [7,8] have investigated the potential of energy storage plants to deliver multiple services to various market participants. In particular, our previous work in reference [8] focused on co-optimizing the provision of multiple services to simultaneously support activities in various sectors in electricity industry.

In terms of battery degradation models, several works have identified the need to incorporate it in economic analysis of electricity systems [9-12]. In particular, references [9-11] focused on battery degradation cost functions that can be included in system optimization models. These approaches have been proposed to investigate effects of either energy arbitrage [10], peak shaving [11] and frequency control services [12] on battery degradation. Hence, although effects of energy storage plant operational decisions on degradation have been already recognized, these are manly based on smaller scale systems and/or a particular application.

A. Contributions

The main contributions of this paper are:

1. A combined economic-degradation model that quantifies effects of various operational policies (which constrain the State-of-Charge (SOC) to specified limits) on gross revenue, multiple services (namely energy arbitrage, balancing services and peak shaving or congestion management), degradation and lifespan of energy storage plants. The proposed economic model (a) presents a simplified (and convex) representation of reactive power that allows us to optimally coordinate active and reactive power for peak shaving purposes, and (b) ensures robustness and deliverability of the committed balancing services.
2. An application on a real 6MW/10MWh Samsung SDI lithium-ion battery system installed in a UK Power Networks' primary substation in London (UK Power Networks owns and operates the distribution network and the storage plant), used to quantify the benefits of various practical operational policies that aim to reduce battery damage. It is demonstrated that although operational policies that focused on battery damage reduction will lead to a revenue loss in the short-term (since these policies fundamentally constrain storage operation), such loss can be more than compensated by long-term revenues due to a lengthier battery lifespan.
3. Demonstration of the effects of ambient temperature fluctuations on storage plant revenue due to degraded capacity

B. Structure

This paper is organized as follows. Section III presents our combined economic-degradation model, whose results and discussions are presented in Section IV. Section V concludes.

III. Combined economic-degradation model

A. Overview

Fig.1 shows a general overview of our proposed approach with (i) an economic-based, commercial strategy module that determines storage plant operation (scheduled and real-time) by optimizing multi-service portfolios of energy storage (network congestion management, energy price arbitrage and various reserve and frequency response services) to maximize gross revenue, and (ii) a degradation module that progressively reduces energy capacity of storage plant as a function of its utilization profile determined in (i). While solution provided by module (i) is sensitive to utilization levels of network infrastructure (i.e. congestion), as well as various prices of energy and balancing services, module (ii)'s solution mainly depends on battery usage (determine by module (i)) and type, besides ambient temperature. As shown in Fig. 1, modules (i) and (ii) are applied on sequential time periods (e.g. week-by-week) that covers a longer time horizon (e.g. several years) as follows:

- Given the storage plant capacity for period p (e.g. a week), module (i) determines optimal economic use of storage capacity within that period (when capacity is considered constant)
- Given the usage profile of storage capacity within period p (determine by module (i)), module (ii) calculates capacity degradation by the end of period p (present week), which is then used as the storage capacity for the optimization of plant operation during next period p + 1 (and this is undertaken in module (i))

Hence, after applications of modules (i) and (ii) over

various and consecutive time periods/weeks (that are part of a longer studied time horizon, e.g. several years), storage plant operation and its capacity degradation can be determined. We use this modeling framework to quantify effects of several operational policies (focused on constraining SOC) on gross revenue, portfolio of services, degradation and life of storage units. Sensitivity to market prices, network congestion levels and temperature are also studied. Note that the degradation module is not embedded in the optimization module and this allows us to carry out a more accurate calculation of degradation.

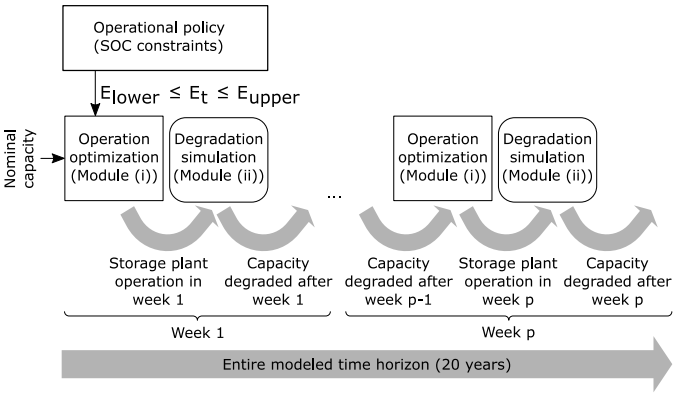

Fig. 1. Overview of proposed economic-degradation model.

B. Economic multi-service operation of storage plant

Storage operation is first scheduled and optimized ahead of real-time and such scheduled operation may change in actual, real-time operation. In this paper, the term storage *scheduled* output refers to the *planned* output which is determined ahead of real-time and is sufficiently robust to cope with the delivery of contracted services, if exercised or called for in real-time. Scheduled output presents a plan of how storage should be operated under the most expected condition (i.e. no utilization of frequency or reserve services) to be able to deliver the contracted levels of services in case exercise is needed. This scheduled or planned output will be different from the *real-time* output since the latter will depend on the actual realizations of the delivery of services that storage is committed to provide. Submodules that determine scheduled and real-time storage operation are presented next.

1) Scheduled operation

This section presents a price-taker profit maximization model to determine uses of distributed storage capacity to provide multiple services to energy and balancing markets and DNO as follows (see Fig. 2):

- Energy price arbitrage, associated with charging/buying at low energy prices and discharging/selling at higher energy prices.
- System balancing services
  - The frequency response services, associated with the fast, automatic response when a system frequency deviation occurs. The upwards and downwards terms refer to the increment (upwards) or decrement (downwards) action to maintain the system's nominal frequency at the required value.
  - The reserve operating services, associated with the slower, centrally controlled demand–supply balance over a longer timescale. The upwards and downwards terms refer to the increment (upwards) or decrement (downwards) action to maintain the supply-demand balance of the whole system.
- DNO peak demand shaving, associated with the congestion management at the primary substation level through active and reactive power control.

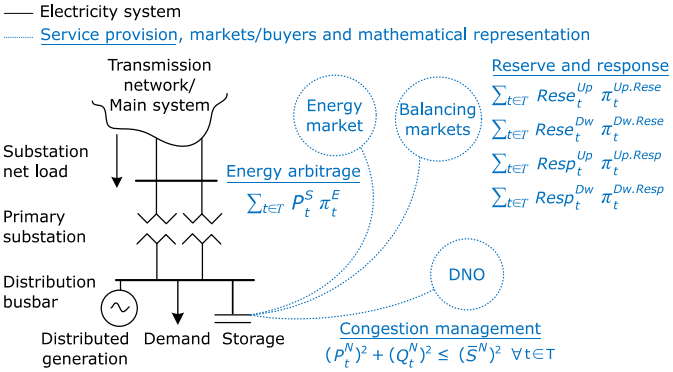

Fig. 2. Diagram of modeled energy storage, demand (including distributed generation) and primary substation along with services buyers.

The developed non-linear model maximizes, through Eq. (1), the overall revenue streams that energy storage could earn, given the set of prices associated with different services, by coordinating delivery of multiple applications while considering a number of constraints that represent inter-dependences among different services, the energy storage constraints and constraints of the local network infrastructure. In our method, we do not consider a full AC power flow representation and instead we model a simplified version that considers reactive power for congestion management purposes only. Hence, voltage support and network losses are not included in our model and this is considered a reasonable assumption to operate this installation since the focus is on coordination of peak shaving services with grid-scale applications of storage such as energy arbitrage and frequency control and the associated degradation levels.

The main equations of this model are shown in Eq. (1)-(16). The objective function (Eq.(1)) maximizes the summation of several revenue streams as follows: energy arbitrage $\sum_{t\in T} P_t^S \pi_t^{\mathrm{E}}$, upwards reserve $\sum_{t\in T} Rese_t^{Up} \pi_t^{\mathrm{Up.Rese}}$, downwards reserve $\sum_{t\in T} Rese_t^{Dw} \pi_t^{\mathrm{Dw.Rese}}$, upwards response $\sum_{t\in T} Resp_t^{Up} \pi_t^{\mathrm{Up.Resp}}$, and downwards response $\sum_{t\in T} Resp_t^{Dw} \pi_t^{\mathrm{Dw.Resp}}$. Note that for frequency control services, revenue depends on the capacity held/reserved to provide the service (availability) regardless of its utilization.

While Eq. (2)-(4) ensure that storage plant actions comply with network infrastructure capacities and eventually alleviates network congestion during peak demand periods, Eq. (5)-(11) ensure that all storage plant capacities in terms of both power and energy are respected, maintaining the needed power capacity margins to provide balancing services (Eq. (10)-(11)). Note that D_t^S and C_t^S cannot take values greater than zero simultaneously since there is a roundtrip efficiency

parameter η in Eq. (8) smaller than 1 that will penalize simultaneous charging and discharging outputs of storage. The model uses reactive power as a measure to reduce network congestion without the need to increase active power injections from storage plant and thus provide peak shaving services more efficiently. Note that Eq. (2) and (7), although non-linear, describe a convex region and thus can be linearized via tangent planes. This allows us to use commercial Mixed Integer Linear Programing (MILP) solvers on the proposed formulation.

Objective function

$$Max\left\{\sum_{t\in T} P_t^S \cdot \pi_t^{\mathrm{E}} + Rese_t^{Up} \cdot \pi_t^{\mathrm{Up.Rese}} + Rese_t^{Dw} \cdot \pi_t^{\mathrm{Dw.Rese}} + Resp_t^{Up} \cdot \pi_t^{\mathrm{Up.Resp}} + Resp_t^{Dw} \cdot \pi_t^{\mathrm{Dw.Resp}}\right\} \quad (1)$$

s.t.

Active and reactive power capacities

$$(P_t^N + Resp_t^{Dw} + Rese_t^{Dw})^2 + (Q_t^N)^2 \le (\overline{S}^{\mathrm{N}})^2 \quad \forall\, t \in T \quad (2)$$

$$P_t^N = P_t^{\mathrm{D}} - P_t^S \quad \forall\, t \in T \quad (3)$$

$$Q_t^N = Q_t^{\mathrm{D}} - Q_t^S \quad \forall\, t \in T \quad (4)$$

$$P_t^S = D_t^S - C_t^S \quad \forall\, t \in T \quad (5)$$

$$-\overline{C}^{\mathrm{S}} \le P_t^S \le \overline{D}^{\mathrm{S}} \quad \forall\, t \in T \quad (6)$$

$$(P_t^S)^2 + (Q_t^S)^2 \le \left(\overline{S}^{\mathrm{S}}\right)^2 \quad \forall\, t \in T \quad (7)$$

Temporal balance constraints

$$E_t = E_{t-1} - (D_t^S - C_t^S \cdot \eta) \quad \forall\, t \in T \quad (8)$$

$$E_t \le \overline{E} \quad \forall\, t \in T \quad (9)$$

Capacity headroom associated with balancing services

$$P_t^S + Rese_t^{Up} + Resp_t^{Up} \le \overline{D}^{\mathrm{S}} \quad \forall\, t \in T \quad (10)$$

$$P_t^S - Resp_t^{Dw} - Rese_t^{Dw} \ge -\overline{C}^{\mathrm{S}} \quad \forall\, t \in T \quad (11)$$

Robustness and deliverability constraints

$$-\mathrm{M}\cdot\left(1 - X_t^{Up.Rese}\right) \le E_{t-1} - \left(P_t^S + \alpha \cdot Rese_t^{Up}\right)\cdot\beta\cdot\tau^{\mathrm{Rese}} \le \overline{E} + \mathrm{M}\cdot\left(1 - X_t^{Up.Rese}\right) \quad \forall\, t \in T, \alpha \in A \quad (12)$$

$$-\mathrm{M}\cdot(1 - X_t^{Dw.Rese}) \le E_{t-1} - (P_t^S - \alpha \cdot Rese_t^{Dw})\cdot\beta\cdot\tau^{\mathrm{Rese}} \le \overline{E} + \mathrm{M}\cdot(1 - X_t^{Dw.Rese}) \quad \forall\, t \in T, \alpha \in A \quad (13)$$

$$Rese_t^{Up} \le \mathrm{M}\cdot X_t^{Up.Rese} \quad \forall\, t \in T \quad (14)$$

$$Rese_t^{Dw} \le \mathrm{M}\cdot X_t^{Dw.Rese} \quad \forall\, t \in T \quad (15)$$

Signs and binary variables

$$\left\{C_t^S, D_t^S, E_t, P_t^{\mathrm{D}}, Q_t^{\mathrm{D}}, Rese_t^{Up}, Resp_t^{Up}, Rese_t^{Dw}, Resp_t^{Dw}\right\} \ge 0 \quad \forall\, t \in T$$

$$\left\{X_t^{Up.Rese}, X_t^{Dw.Rese}\right\} \in \{0,1\} \quad (16)$$

When selecting the portfolio of services, the proposed model will ensure the robustness of delivery against potentially different levels of utilization of stored energy associated with balancing services provided. In other words, the model will always ensure real-time deliverability of services that are scheduled ahead of real-time. For example, if storage is scheduled to provide 1 MW of operating upwards reserve for 2 hours, the model reserves 1 MW of capacity headroom (Eq. (10)) and also sufficient amounts of energy stored (Eq. (12)) to maintain a fixed output ($P_t^S + Rese_t^{Up}$in the worst case, i.e. $\alpha = 1$) while the reserve service is exercised (during 2 hours in the worst case, i.e. $\beta = 1$). To do so, we expanded on our previous disjunctive approach used in [8] to limit the levels of energy stored and thus be able to deliver a scheduled balancing service in real-time (which is ensured by Eq. (12)-(15)), where M is a large number and A is a set of numbers from 0 to 1 that makes scheduled output robust (for the sake of simplicity, Eq. (12)-(15) are only shown for reserve services, but the same constraints applies to frequency response services). α and β are parameters that make the scheduled output more robust against the exercise of balancing services in real-time. For example, $\alpha = 1$ and $\beta = 1$ maintains energy stored so as to deal with the worst cases (e.g. utilization of the maximum reserve capacity $-\alpha = 1-$ persistently for the maximum possible duration of the service $-\beta = 1-$). In contrast, $\alpha = 0$ and $\beta = 0$ does not ensure sufficient levels of energy stored for the purpose of frequency control services. In this context, it is possible to set α and β differently for frequency response and reserve services.

To provide frequency control services, we need to maintain both power capacity headroom and sufficient levels of stored energy. The latter needs binary variables to be properly modeled since energy requirements for frequency control services are not convex. Indeed, extremely small capacity requirements of a frequency control service can drive large requirements of energy stored if the initial position of storage output (before a frequency control service is exercised) is sufficiently high. For example, if the initial output position of storage is equal to +1 MW and then 2 MW of upwards reserve is exercised during 2 hours, the volume of energy stored prior to the utilization of the service has to be at least (1+2) x 2 = 6 MWh (note that when a frequency control service is exercised, the output of storage is kept fixed until the end of the service). The needed volume of energy stored as a function of the booked reserve capacity is shown in Fig.3.

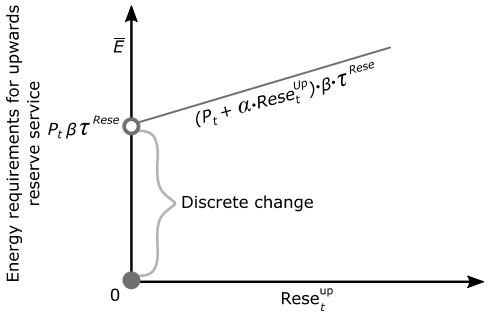

Fig. 3. Energy requirements to deliver upwards reserve service as a function of the committed reserve capacity.

The optimization module also contains further constraints to force volumes of balancing services to remain constant across prescribed time windows (especially defined by system operators to provide balancing services and that cannot be modified or optimized by storage owners) and this will be illustrated later in Section IV.

It is important to emphasize that the optimization model is run over a longer time period (twice longer than the needed time, e.g. 2 weeks), and solution is considered valid only during the first half of the time period modeled (e.g. 1 week). This is done to avoid arbitrary definitions on levels of energy stored at the end of the modeled time period.

2) Real-time operation of storage plant

Once scheduled output is obtained through Eq. (1)-(16),

real-time storage plant operation will be determined by a simulation process that exercises the balancing services committed by the above scheduling submodule. The exercise of a balancing service occurs at a given rate per period, e.g. 7 occurrences per week, and this is defined as a parameter for each balancing service. This case study aims to analyze the impact of changing the real-time output on a daily basis (e.g. 7 times per week) due to a system operator's instruction, and how the lifespan of the storage system is affected. The results associated with the periodic exercise of balancing services are detailed in Section IV.E.

After a balancing service is exercised in real-time, storage plant will rapidly return to the scheduled energy stored levels by implementing a set of charge or discharge actions in real-time that will minimize the time exposure to imbalance fees (paid when a plant presents an imbalance between scheduled and real-time power output). The algorithm that generates real-time outputs of storage plants (from a given scheduled output) is described next. In addition, the algorithm is illustrated in Fig. 4:

- Loop over all t
  - If a balancing service is not exercised in t and battery is not in recovery status: define real-time power output P_t^{RT} equal to scheduled power output P_t. Similarly, define real-time energy stored E_t^{RT} equal to scheduled energy stored E_t.
  - Else if a balancing service is exercised in t: define P_t^{RT} equal to $P_{tr} + \Delta P_{tr}$ where ΔP_{tr} represents a positive (up) or negative (down) imbalance associated with the scheduled/committed balancing service (*tr* is the first hour when a balancing service is exercised; note that during the exercise time, power output of storage remains constant). Apply Eq.(8) to obtain real-time energy stored E_t^{RT}. If this is the last hour t when a balancing service is exercised, set battery in recovery status from t+1.
  - Else if a balancing service is not exercised in t and battery is in recovery status and $E_{t-1}^{RT} \neq E_{t-1}$: define P_t^{RT} equal to the difference between E_{t-1}^{RT} and E_t (note that if storage is charging, aforementioned difference should be divided by η). If this exceeds the power capacity of storage plant, define P_t^{RT} equal to the power capacity.
  - Else if a balancing service is not exercised in t and battery is in recovery status and $E_t^{RT} = E_t$: unset battery in recovery status and define real-time power output P_t^{RT} equal to scheduled power output P_t. Similarly, define real-time energy stored E_t^{RT} equal to scheduled energy stored E_t.
  - End-if
- End-loop

The above algorithm takes into account: (i) an initial normal state (when the storage plant is not providing/utilizing balancing services in real-time), (ii) an exercise state (when the storage plant provides balancing services), (iii) a recovery state (right after a balancing service has been utilized when the storage plant needs to recover SOC levels stated in the planned operation), (iv) and a normal state after the recovery state.

Note that while there is a single scheduled output that is optimal ahead of real-time, an array of real-time outputs can be generated depending on how actual service utilization conditions evolve. The time when a scheduled balancing service is exercised, is a given parameter to the above algorithm and this is used to run a number of sensitivities to study how utilization of services impacts on energy capacity degradation.

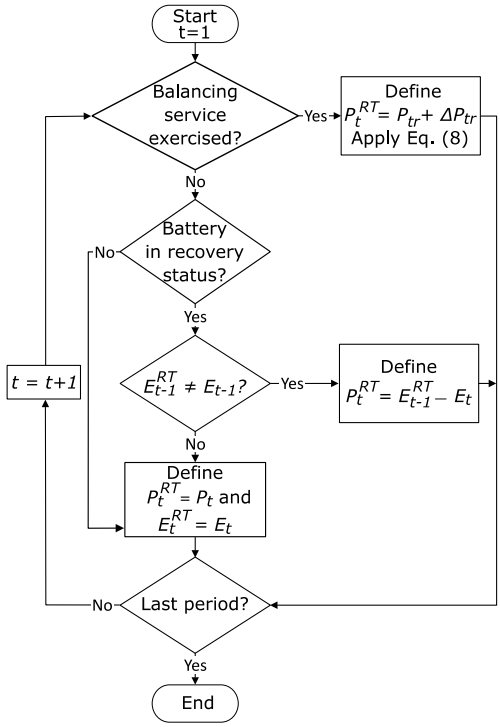

Fig. 4. Generation of real time outputs

C. Energy capacity degradation of storage plant

The concept of battery aging is typically related to the progressive reduction in the amount of energy that can be delivered by the energy storage plant or the growth of its internal impedance. Battery aging is a function of the elapsed time since the manufacture date, as well as the usage over consecutive charge and discharge actions. This work primarily focuses on the latter aspect (which is closely entangled with the problem of economic multi-service operation of storage plants), characterizing usage cycles according to their swing ranges (defined by the minimum and maximum values reached, during a usage cycle, by the battery SOC [13-16]). The proposed algorithm for computing overall capacity degradation over a given period (e.g. 1 week) is divided into 3 sections (or submodules) that are run sequentially as follows: (1) cycle length calculation, (2) cycle characterization and energy capacity degradation, and (3) temperature modulation (see Fig. 5).

1) Cycle length calculation

The purpose of this submodule is to determine the duration of each of the usage cycles that are present in a given operation profile. In this paper, a usage cycle is defined either by a charge action (or several successive charge actions) followed by a discharge action, or a discharge action (or

several successive discharge actions) followed by a charge action. To find these patterns, we use P_t to recognize when a cycle starts and finishes by using the algorithm described next (that fundamentally finds each cycle based on changes in the sign of P_t). The algorithm below is also illustrated in Fig. 6.

- Loop over all t
  - If a usage cycle has not been defined in t:
    - If $P_t = 0$, goto End-if(1)
    - Else if $P_t > 0$: define usage cycle as discharge/charge.
    - Else if $P_t < 0$: define usage cycle as charge/discharge.
    - End-if
  - Else
    - If usage cycle is discharge/charge type and $P_{t-1} < 0$ *and* $P_t \geq 0$: usage cycle is set as finished in t-1 and a new usage cycle is started in t and set as undefined.
    - Else if usage cycle is charge/discharge type and $P_{t-1} > 0$ *and* $P_t \leq 0$: usage cycle is set as finished in t-1 and a new usage cycle is started in t and set as undefined.
    - End-if
  - End-if(1)
- End-loop

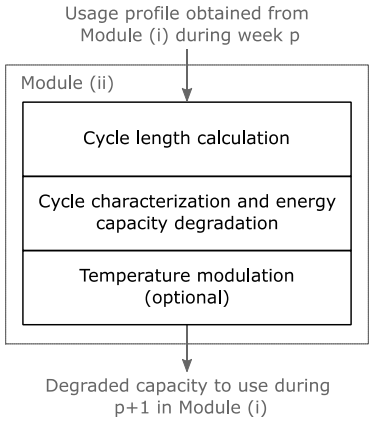

Fig. 5. Submodules of the proposed algorithm. Module (i) and (ii) are those illustrated in Fig.1.

The above algorithm will determine complete and partial charge/discharge usage cycles, which will degrade storage capacity differently, in terms of their characterization.

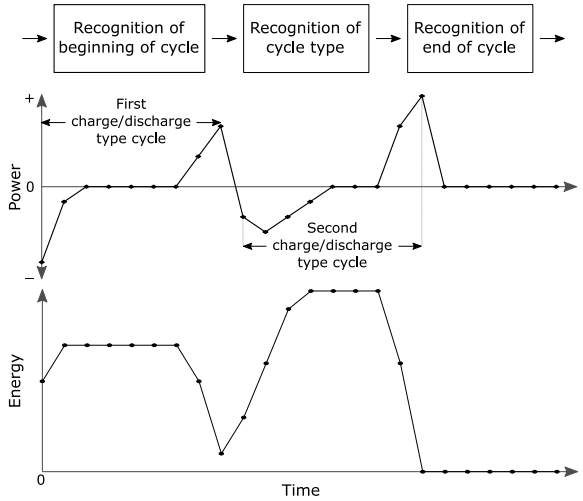

Fig. 6. Cycle recognition.

2) Cycle characterization and degradation

The degradation model is based on the structure proposed in [17], which corresponds to an extension of the model used in [18]. Every cycle identified in the aforementioned submodule is characterized now in terms of the associated Coulombic efficiency ($\bar{\bar{\eta}}_k$). The value of this parameter corresponds to a measure of the expected capacity loss per cycle (as a percentage of the capacity offered by the battery during the previous discharge cycle). The Coulombic efficiency is used to degrade storage capacity after a cycle k through Eq. (17).

$$\bar{\bar{E}}_{k+1} = \bar{\bar{\eta}}_k \bar{\bar{E}}_k \tag{17}$$

To calculate $\bar{\bar{\eta}}_k$, we use data provided by manufacturer that characterizes the battery lifespan (i.e. number of cycles) when storage plant is sequentially charged and discharged at rated current, and following strict protocols that ensure specific swing ranges (11 swing ranges were provided: 0-25%, 0-50%, 0-75%, 0-100%, 25-100%, 50-100%, 75-100%, 25-50%, 25-75%, 50-75%, and 37.5-62.5%). We also assume that battery can be used up to when degraded capacity reaches 75% of the initial, nominal capacity. This assumption is actually a standard practice, as explained in [17], which is justified by the growth of battery internal resistance (as battery cells degrade) and the subsequent increment in heat losses. Although dataset provided was comprehensive, this does not cover all possible swing ranges that may occur in practice and thus we use Similarity Based Modelling (SBM [19]) to interpolate and obtain the most appropriate value for the Coulombic efficiency $\bar{\bar{\eta}}_k$ that can be used for an observed swing range. In this case, SBM is applied by choosing the three nearest neighbors of the actual operating condition (described by a SOC swing –the difference between the initial value of the SOC at the beginning of a cycle and the final value of the SOC once the cycle is over– and an average swing range –the average of (i) the initial value of the SOC at the beginning of a cycle and (ii) the final value of the SOC once the cycle is over–) of each cycle, to the given conditions by the manufacturer, and using the inverse of the distances between those neighbors to compute a weight. The weighted average of the values for $\bar{\bar{\eta}}_k$ that better represent the three nearest neighbors is the value for the Coulombic efficiency that will be used on our model for that particular discharge cycle.

It is critical to emphasize here a few important facts related to battery degradation and the operating conditions informed by the manufacturer. On the one hand, capacity fade is typically accelerated by operating profiles that offer a combination of high average SOC levels, deep discharges, extremely high or low temperatures, and overcharging [20]. On the other hand, operating a battery with low average SOC (e.g., SOC swing ranges between 0-25%) can be beneficial in terms of incrementing the lifespan [21]. Nevertheless, the latter statement is only valid when avoiding cell over-discharge, or when the user does not store the battery discharged for an extended period of time (a procedure that leads towards permanent cell damage, because self-discharge

phenomena can cause cell over-discharge). In this regard, when forcing operation at low SOC values it is important to differentiate between deep discharges (accelerated degradation) and small SOC swing ranges.

So far, temperature is assumed to be nominal and equal to 25°C, a credible assumption if we accept incurring in expenses associated with temperature control systems. In the next section, we show how variations in temperature can be addressed in the analysis (this is used for sensitivity).

3) Temperature modulation

It is a well known fact [22] that the battery degradation trend will not be a function of temperature, as long as the ranges suggested by the manufacturer are observed. Nevertheless, the actual amount of energy delivered (or stored) by the battery during a specific usage cycle will definitively be a function of the operating temperature [23]. The relation between the actual amount of energy delivered by a lithium-ion battery during a cycle and the average temperature is characterized by Eq. (18) (Vogel-Tammann-Fulcher –VTF–, suggested in [24]). This expression (empirically tested and validated) allows to incorporate the concept of "usable capacity" [24], which corresponds to the amount of energy that the battery can deliver (or store) during a cycle, assuming an average temperature T.

Eq. (18) allows us to consider the effect of ambient temperature on energy storage capacity, empirically determining multiplying factors that can be applied on degraded capacity $\bar{\bar{E}}_k$ (which is calculated at nominal temperature, i.e. 25°C, as explained in the previous section) to further reduce or increase energy capacity of a storage plant that is not subject to temperature control.

$$\hat{E}_k = \bar{\bar{E}}_k e^{-\mu\left(\frac{1}{T-\gamma}-\frac{1}{T^{nom}-\gamma}\right)} \quad (18)$$

μ and γ are determined through data provided by battery cell manufacturer, using maximum likelihood estimators.

Note that we used the ambient temperature as the main indicator to modulate energy storage capacity. This choice is based on two main assumptions. The first one is that, the cooling system forces air into the battery pack in an effort to reduce temperature, avoiding to incur in costs associated with full temperature control (i.e., a system that would aim at keeping temperature constant). The second assumption is that the battery pack is most of the times in idle mode (neither charging nor discharging), allowing it to cool the cells using the aforementioned air flow. Indeed, even when the battery pack is used intensively (swing range of 0-100%), it rests in idle mode approximately 63.25% of the time. Other cases even imply being in idle mode for 83% of the time.

IV. Results and Discussion

A. Input data

Time series with hourly resolution of GB system energy prices and demand at one of the distribution network substation in London (Leighton Buzzard) are used in this paper to optimize the storage plant operation. We also assume a fixed price for frequency response and reserve services of 7 and 6 £/MW/h, respectively, and a service prescribed time window between 4:00h and 8:00h for frequency response services, and between 16:00h and 21:00h for reserves. If a balancing service is exercised, its maximum duration cannot exceed 30min and 2h for frequency response services and reserves, respectively (i.e. $\tau^{\mathrm{Rese}} = 2\mathrm{h}$ and $\tau^{\mathrm{Resp}} = 0.5\mathrm{h}$). Additionally, we assume that balancing services are cleared in a weekly auction, which leads to a constant committed volume of each balancing service for all prescribed windows in a week.

The main data of storage plant used in the model is as follows:

- Storage power and energy capacity: 6MW, 7.5 MVA, and 10 MWh
- Round trip efficiency: 85%
- Primary substation N-1 capacity: 36 MVA

To obtain the hourly scheduled output of a storage plant for a given operational policy (e.g. SOC within 0-25%) during 20 years, the optimization model is run 1,043 times since every week is optimized in separated and sequential simulations (there are 1,043 weeks in 20 years). Weeks are optimized sequentially (i.e. one after another) in order to determine the level of degradation after every week, which will affect the energy capacity of storage ($\bar{\mathrm{E}}$) to be used in the optimization of the next week. In the optimization of storage operation within week k, the initial SOC used is equal to that obtained at the end of week k-1 (it is important to emphasize that the optimization model is run over a longer time period –twice longer than the needed time, e.g. 2 weeks–, and the solution is considered valid only during the first half of the time period modeled, e.g. 1 week, and this is done to avoid arbitrary definitions on stored energy levels at the end of the modeled time period).

Next, we run several case studies under various future scenarios in the long-term (e.g. 20 years). Future scenarios are built by using 2-year historical data provided by UK Power Networks and time series analysis as follows:

- We build a base case of demand and energy prices across 20 years (used in Section IV.B-F) by repeating the 2-year historical data provided
- We build a time series of the daily ambient temperature across 20 years (used only for sensitivity analysis in Section IV.F) by using the methodology proposed in [25] and the historical data published in [26]
- We build 10 scenarios of demand requirements across 20 years (used in Section IV.G) by fitting a time series model that then produced 10 synthetic, future scenarios
- We build 10 scenarios of energy prices across 20 years (used in Section IV.G) using an economic dispatch model that simulates 10 different generation capacity expansion scenarios in GB

Note that the time series models used are outside the scope of this paper and they can be replaced by another forecast technique that properly captures the statistical characteristics of the data historically observed.

B. Storage economics and degradation in a week

This section aims at illustrating and validating the method used in the paper to optimize operation, and calculate gross revenue and degradation of a storage plant within a week. In this context, Fig 7. shows power outputs and stored energy levels for both scheduled and real-time operation of storage plant.

Scheduled output shown in Fig. 7 is optimized for the provision of multiple storage applications or services: energy arbitrage (162£/day by buying in the morning between 2:00h and 3:00h a total volume of 8MWh at an average price of 35£/MWh and selling in the evening between 22:00h and 23h a total volume of 6.8MWh at an average price of 65£/MWh with a 85% efficiency), frequency response (420£/day by holding 6MW of each upwards and downwards service in the morning between 4:00h and 8:00h at a price of 7£/MW/h), and reserve (180£/day by holding 3.4MW of upwards service and 1.6MW of downwards service in the afternoon between 16:00h and 21:00h at a price of 6£/MW/h –note that services are constrained by SOC at that time, which is equal to 6.8MWh–). This degrades capacity from 10MWh to 9.996781MWh due to occurrence of 7 partial cycles within a swing range between 0% and 68%, each with a Coulombic efficiency of 0.999954. If a balancing service is exercised every day during that week (which can potentially occur in real-time operation as shown in Fig. 7), this would degrade capacity further from 10MWh to 9.993562MWh due to occurrence of 14 partial cycles within a swing range between 0% and 68%. Note that utilization of balancing services may not necessarily increase the number of cycles (as in the case above), but rather expand the swing range of charge/discharge actions.

This demonstrates that reserving capacity for balancing services may be detrimental in terms of degradation, depending on how frequent these services will be exercised by the system operator (and this will be analyzed in more detail in Section IV.E). Fig.7 also shows that scheduled operation determined by the proposed model (Eq. (1)-(16)) is robust against real-time utilization of balancing services (i.e. deliverable in real-time).

C. Effect of operational policies

Data provided by manufacturer suggest that battery lifespan can be significantly increased if plant is operated within a smaller swing range (e.g. 0-25%) rather than within its full energy capacity (e.g. 0-100%). Hence, we calculate revenues and degradation associated with 11 operational policies that aim at constraining SOC. To do so, we added lower and upper limits to E_t in the scheduling submodule in order to constrain SOC to a given range.

In this context, Fig. 8 shows that constraining SOC when deciding optimal operation of storage plant presents clear benefits, since battery lifespan can be more than doubled. For example, battery lifespan lasts about 76,000h if SOC is unconstrained, which can be increased up to more than 175,000h if SOC is constrained between 0 and 25%. Another interesting feature, shown in Fig. 8, is that it is more attractive to limit upper rather than lower bounds of the swing range. In fact, increasing lower bounds may decrease battery lifespan with respect to the unconstrained case (i.e. 0-100%) and this is consistent with manufacturer data.

The above benefits are in opposition to short-term revenues. In fact, constraining SOC between 0 and 25%, for instance, can present about 18% lower gross revenue levels per year as shown in Fig. 9 (where results are sorted in decreasing order).

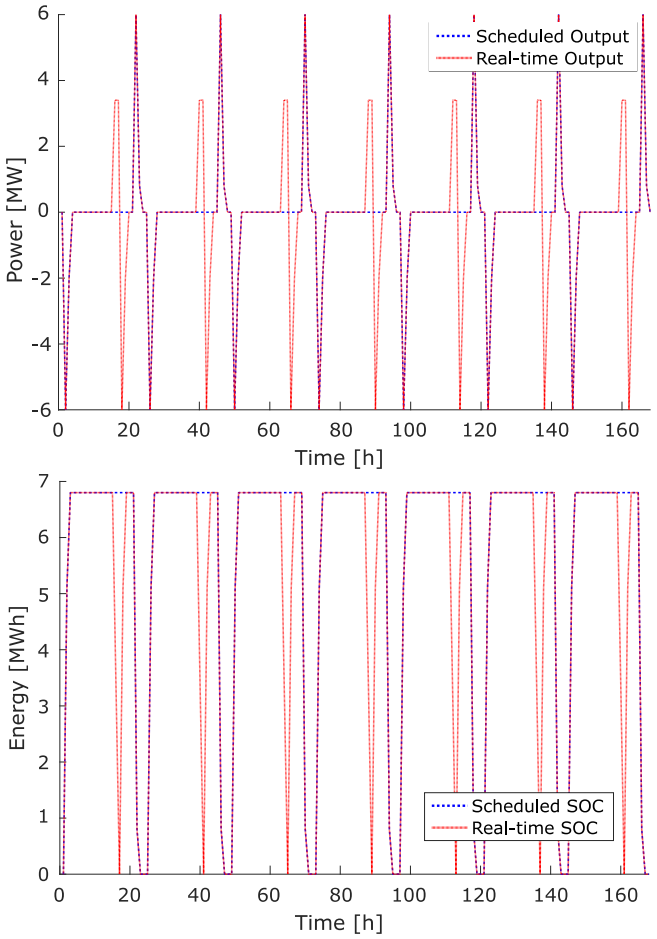

Fig. 7. Schedule and one potential real-time power output (top) and SOC (bottom).

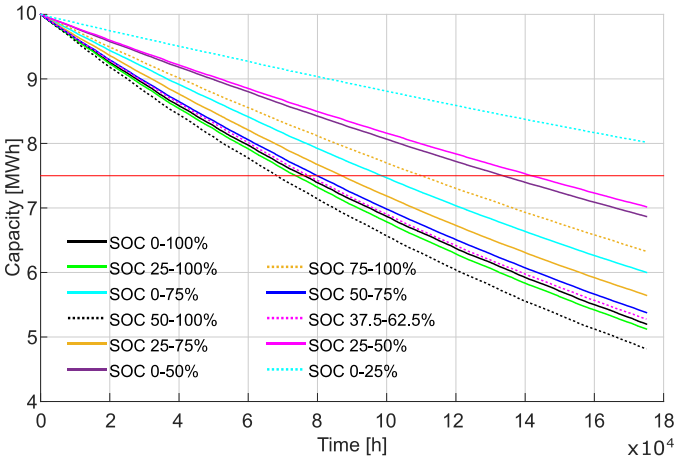

Fig. 8. Energy capacity degradation for different operational policies. Horizontal red line indicates 75% of the nominal energy capacity.

Despite this, lower average gross revenues (in £/annum) can be compensated by revenue streams in the longer term that are associated with a lengthier lifespan of storage plant and this is shown in Fig. 10 (where results are sorted in decreasing order). Effectively in this GB case study, it is clearly more beneficial to constrain the SOC scheduled output since its benefits in terms of battery lifespan increase, more than compensate the revenue loss in the short-term incurred in energy and balancing markets. In fact, for the 0-25% policy, lifespan increase (i.e. >+100%) is clearly disproportionally higher than reduction in gross revenue (i.e. ~ –18 %).

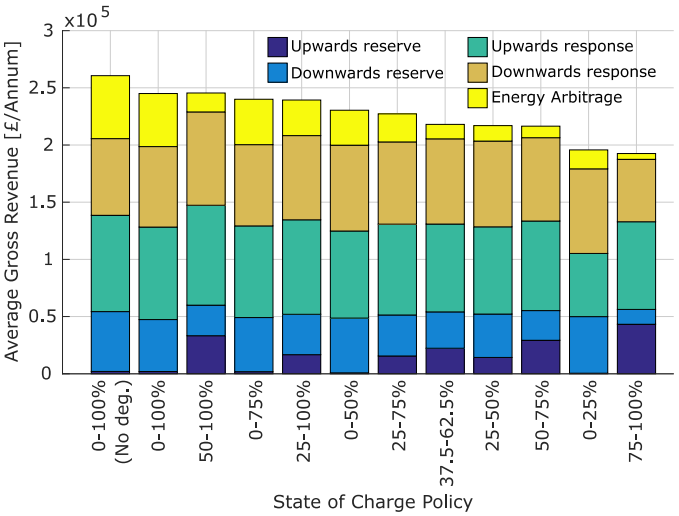

Fig. 9. Average annual gross revenue during battery lifespan (no discount rate). "No deg." refers to no degradation (where operation is optimized during 20 years without degradation and this case is used as a benchmark).

D. Effect on multi-service portfolios

Fig. 11 (where results are sorted in decreasing order) suggests that all operational policies affect revenues in the short-term and that this is mainly driven by revenue changes in services that are more energy intensive such as energy and reserve, while revenue streams associated with frequency response services are more stable.

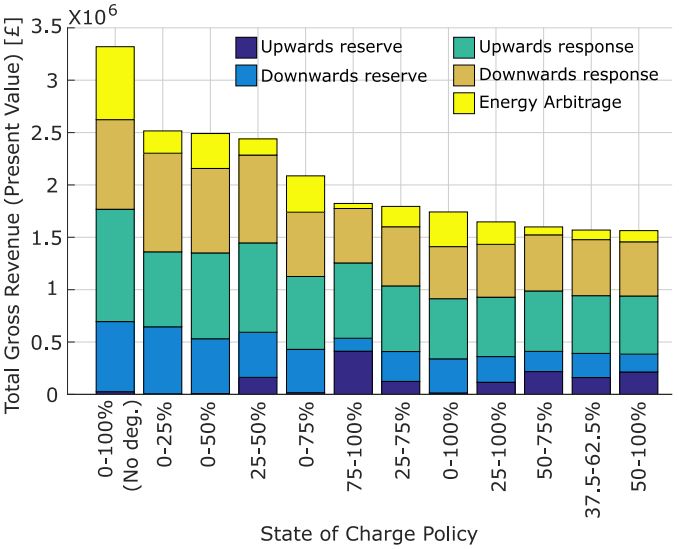

Fig. 10. Total gross revenue during battery lifespan (5% discount rate).

Furthermore, Fig. 11 also demonstrates that revenues associated with balancing services do not necessarily decrease when SOC is constrained to improve battery lifespan. In fact, as energy arbitrage is limited when SOC is constrained, there are capacity margins of storage plant that can be used for further services. Therefore, short-term revenue losses associated with operational policies that aim at increasing battery lifespan, will ultimately depend on energy and balancing markets conditions and can be limited if storage capacity is used for application in balancing rather than energy market.

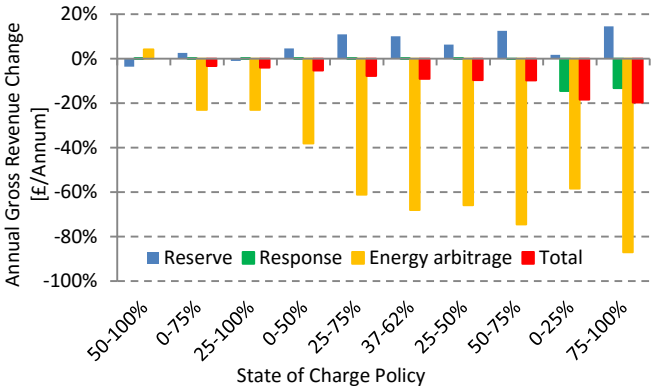

Fig. 11. Average annual gross revenue change with respect to 0-100% policy.

E. Effect of balancing services utilization in real-time on battery lifespan

We model two cases without and with utilization of balancing services for all operational policies when considering an exercise rate of one service per day, and this demonstrates that battery lifespan can be reduced by 28% in the worst case. These results are shown in Table I.

Table I also demonstrates that reserving capacity for balancing services may be detrimental, depending on how frequent these services will be exercised by the system operator and this affects large majority of operational policies. Interestingly, 0-25% policy (which is the most profitable policy and that with the lengthiest lifespan) is not affected.

TABLE I
Battery lifespan with and without balancing services utilization/exercise

SOC Policy	Balancing service utilization [h]	No balancing service utilization [h]	Reduction [h]	Reduction [%]
25-100%	52759	73738	-20979	-28%
37-62%	55517	77388	-21871	-28%
0-50%	96050	133479	-37429	-28%
0-100%	54987	76164	-21177	-28%
0-75%	71776	98531	-26755	-27%
25-75%	65067	87014	-21947	-25%
50-100%	52395	68200	-15805	-23%
25-50%	110717	141685	-30968	-22%
50-75%	64186	79887	-15701	-20%
75-100%	93638	109981	-16343	-15%
0-25%*	175200	175200	0	0%

*Modeled lifespan in both cases exceed figure provided by manufacturer

F. Effect of temperature control

We model effect of energy capacity changes due to ambient temperature in the absence of controls that can maintain it constant at its nominal value (i.e. 25°C). We use daily temperatures based on historical data that is publicly available at the site of the storage plant (which can be found in [26]) to fit a time series model that can produce stochastic scenarios of temperatures up to 20 years. The time series was generated by using the method proposed in [25]. Fig. 12, that shows energy capacity excursion of 3 operational policies compared with those obtained in Section IV.C at nominal temperature, demonstrates that capacity can be significantly reduced during winter (below 75%), even during the firsts years of operation.

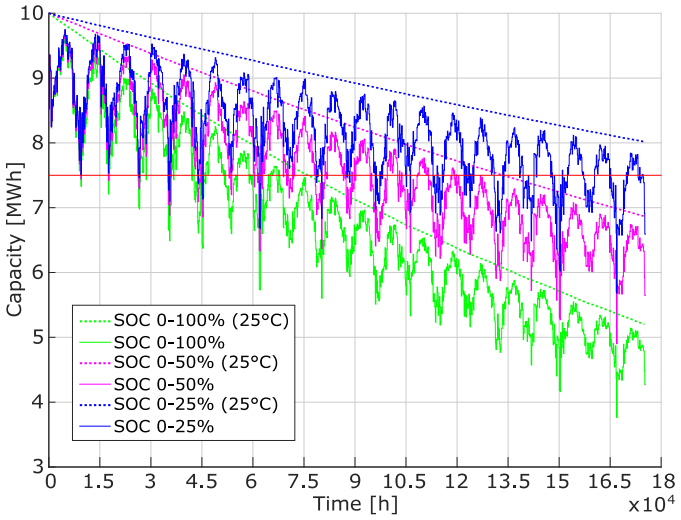

Fig. 12. Energy capacity degradation for 3 operational policies with (solid lines) and without (dotted lines) temperature control. Horizontal red line indicates 75% of the nominal energy capacity.

Despite this and in line with results in previous sections, we found that effect of temperature on gross revenues is limited to about -3% due to market conditions in GB. In effect, capacity reduction due to temperature mainly affects revenues associated with the energy market (about -9%), which is less attractive than further balancing markets whose revenues are less dependent on fluctuations in capacity due to temperature and this is demonstrated in Fig. 13.

G. Sensitivities to demand and prices

We run various sensitivities to study robustness of the above results with respect to future changes in demand and prices. To do so, we use the 10 scenarios of demand and the 10 scenarios of energy prices explained in Section IV.A.1. This analysis was performed only for the 0-100% SOC policy and at the nominal temperature of 25°C. In this context, results proved robust and changes in battery lifespan were below 5% as shown in Fig. 14.

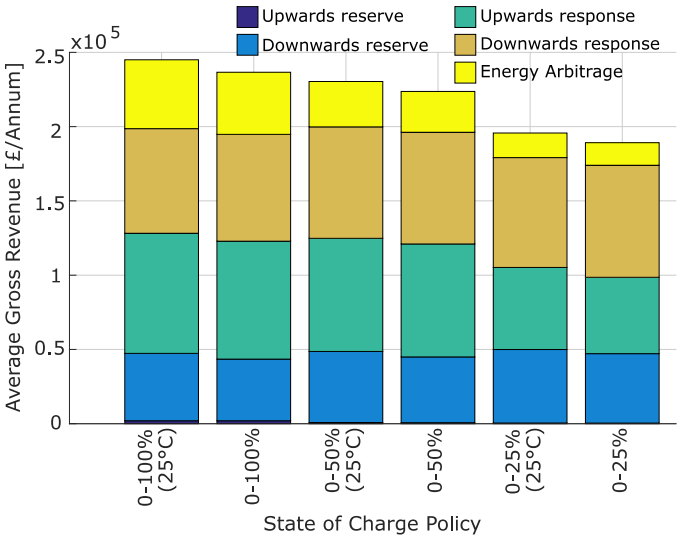

Fig. 13. Comparison of average annual gross revenue during battery lifespan with and without temperature control (no discount rate).

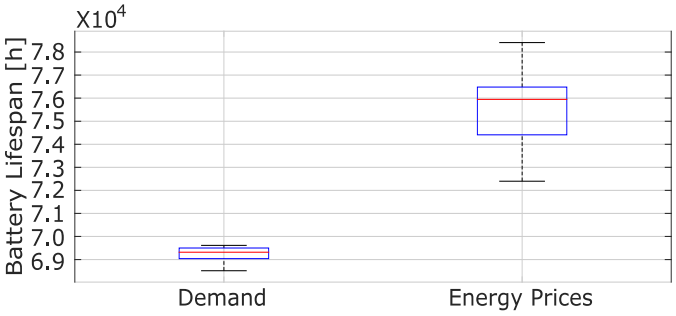

Fig. 14. Sensitivity analysis for 10 scenarios of future demand and energy price time series (0-100% operational policy).

V. Conclusions

We developed a combined economic-degradation model to quantify effects of various operational policies (mainly focused on constraining SOC to prescribed levels) on gross revenue, multi-service portfolios, degradation and lifespan of energy storage plants. We also used the model to demonstrate conflicts and synergies of different storage applications with battery degradation. In particular, we demonstrated that although operational policies focused on battery damage reduction will lead to a revenue loss in the short-term (since these policies fundamentally constrain storage operation), such loss can be more than compensated by long-term revenues due to a lengthier battery lifespan. In the case of GB, for instance, constraining SOC to a swing range between 0 and 25% has the potential to increase total gross revenues up to circa 44% (across the entire lifespan and considering a discount rate of 5%). Additionally, we demonstrated that short-term revenue losses associated with the application of operational policies are mainly driven by revenue reduction in the energy rather than balancing market. Furthermore, this reduction in energy services can lead to both increase in balancing services (since there are more capacity margins available) and decrease in battery capacity degradation. Despite this, increased utilization rates of balancing services by system operators can be

detrimental for storage plants and reduce battery lifespan (which can apply to any operational policy). Finally, we demonstrated that variations of ambient temperature have the potential to decrease storage plants owners' profits (especially in winter), albeit it is not significant in the case of GB (although we recognize that this is dependent on market conditions and on how attractive the energy market is against balancing services markets).

This work can promote efficient integration of new distributed storage projects and provide insights associated with the development of efficient operational policies to ensure that storage plants are adequately operated by balancing both short and long-term costs and benefits, and thus that investors in storage plants are efficiently rewarded for the delivery of value to multiple electricity sectors.

VI. References

[1] M. Black and G. Strbac, "Value of Bulk Energy Storage for Managing Wind Power Fluctuations," *Energy Conversion, IEEE Transactions on,* vol. 22, pp. 197-205, 2007.

[2] C. A. Hill, M. C. Such, C. Dongmei, J. Gonzalez, and W. M. Grady, "Battery Energy Storage for Enabling Integration of Distributed Solar Power Generation," *Smart Grid, IEEE Transactions on,* vol. 3, pp. 850-857, 2012.

[3] E. Drury, P. Denholm, and R. Sioshansi, "The value of compressed air energy storage in energy and reserve markets," *Energy,* vol. 36, pp. 4959-4973, 2011.

[4] L. Ning, J. H. Chow, and A. A. Desrochers, "Pumped-storage hydro-turbine bidding strategies in a competitive electricity market," *Power Systems, IEEE Transactions on,* vol. 19, pp. 834-841, 2004.

[5] K. Bradbury, L. Pratson, and D. Patiño-Echeverri, "Economic viability of energy storage systems based on price arbitrage potential in real-time U.S. electricity markets," *Applied Energy,* vol. 114, pp. 512-519, 2014.

[6] P. Denholm and R. Sioshansi, "The value of compressed air energy storage with wind in transmission-constrained electric power systems," *Energy Policy,* vol. 37, pp. 3149-3158, 2009.

[7] D. Pudjianto, M. Aunedi, P. Djapic, and G. Strbac, "Whole-Systems Assessment of the Value of Energy Storage in Low-Carbon Electricity Systems," *Smart Grid, IEEE Transactions on,* vol. 5, pp. 1098-1109, 2014.

[8] R. Moreno, R. Moreira, and G. Strbac, "A MILP model for optimising multi-service portfolios of distributed energy storage," *Applied Energy,* vol. 137, pp. 554-566, 2015.

[9] M. Koller, T. Borsche, A. Ulbig, and G. Andersson, "Defining a degradation cost function for optimal control of a battery energy storage system," in *PowerTech (POWERTECH), 2013 IEEE Grenoble*, 2013, pp. 1-6.

[10] S. B. Peterson, J. Apt, and J. F. Whitacre, "Lithium-ion battery cell degradation resulting from realistic vehicle and vehicle-to-grid utilization," *Journal of Power Sources,* vol. 195, pp. 2385-2392, 2010.

[11] W. Yanzhi, L. Xue, X. Qing, C. Naehyuck, and M. Pedram, "Minimizing state-of-health degradation in hybrid electrical energy storage systems with arbitrary source and load profiles," in *Design, Automation and Test in Europe Conference and Exhibition (DATE), 2014*, 2014, pp. 1-4.

[12] E. Ju-Kyoung, L. Soon-Ryung, H. Eun-Jung, C. Bong-Yeon, and W. Chung-Yuen, "Economic dispatch algorithm considering battery degradation characteristic of energy storage system with PV system," in *Electrical Machines and Systems (ICEMS), 2014 17th International Conference on*, 2014, pp. 849-854.

[13] M. Daigle and C. Kulkarni, "Electrochemistry-based battery modeling for prognostics," *in 2013 Annual Conference of the Prognostics and Health Management Society*, pp. 249–261.

[14] G. Ning, R. E. White, and B. N. Popov, "A generalized cycle life model of rechargeable Li-ion batteries," *Electrochimica Acta,* vol. 51, pp. 2012-2022, 2006.

[15] D. Haifeng, W. Xuezhe, and S. Zechang, "A new SOH prediction concept for the power lithium-ion battery used on HEVs," *in Proc. 2009 IEEE Vehicle Power and Propulsion Conf.*, pp. 1649–1653. 2009.

[16] T. Guena and P. Leblanc, "How Depth of Discharge Affects the Cycle Life of Lithium-Metal-Polymer Batteries," *in 2006 Annual International Telecommunications Energy Conf. (INTELEC '06)*, pp. 1–8.

[17] B. E. Olivares, M. A. Cerda Munoz, M. E. Orchard, and J. F. Silva, "Particle-Filtering-Based Prognosis Framework for Energy Storage Devices With a Statistical Characterization of State-of-Health Regeneration Phenomena," *IEEE Trans. Instrumentation and Measurement*, vol. 62, pp. 364–376, 2013.

[18] B. Saha and K. Goebel , "Modeling Li-ion Battery Capacity Depletion in a Particle Filtering Framework," in *Proc. 2009 Annual Conference of the Prognosis and Health Management Society,* pp. 2909-2924.

[19] L. Gong and D. Schonfeld. "Space Kernel Analysis," *in Proc.2009 IEEE International Conference on Acoustics, Speech and Signal Processing*, pp. 1577-1580.

[20] J. Vetter, P. Novák, M.R. Wagner, C. Veit, K.C. Möller, J.O. Besenhard, A. Hammouche, "Ageing mechanisms in lithium-ion batteries," *Journal of Power Sources*, vol. 147, pp. 269–281, 2005. http://doi.org/10.1016/j.jpowsour.2005.01.006

[21] Q. Xie, X. Lin, Y. Wang, M. Pedram, D. Shin, and N. Chang, "State of health aware charge management in hybrid electrical energy storage systems," *in 2012 IEEE Design, Automation & Test in Europe Conference & Exhibition (DATE)*, pp. 1060-1065.

[22] C. Zhou, K. Qian, M. Allan, and W. Zhou, "Modeling of the Cost of EV Battery Wear Due to V2G Application in Power Systems," *IEEE Trans. Energy Conversion*, vol. 26, pp. 1041–1050, 2011.

[23] A. Millner, "Modeling Lithium Ion battery degradation in electric vehicles," *in 2010 IEEE Conf. on Innovative Technologies for an Efficient and Reliable Electricity Supply (CITRES)*, pp. 349–356.

[24] L. Lam, P. Bauer, and E. Kelder, "A practical circuit-based model for Li-ion battery cells in electric vehicle applications," *in 2011 IEEE 33rd International Telecommunications Energy Conference (INTELEC)*, pp.1-9.

[25] V. Badescu, *Modeling Solar Radiation at the Earth Surface*, Springer-Verlag, pp. 282, 2008.

[26] Weather.org. [Online]. Available: http://weather.org/weatherorg_records_and_averages.htm

Aramis Perez has a B.Sc. degree in Electrical Engineering and a M.Sc. degree in Business Administration from the University of Costa Rica. He is currently a Doctorate Student at the Department of Electrical Engineering and a Research Assistant at the Lithium Innovation Center in the University of Chile, and an Assistant Professor at the School of Electrical Engineering in the University of Costa Rica. His research interests include parametric/non-parametric modeling, system identification, data analysis, machine learning and manufacturing processes.

Rodrigo Moreno (M'05) has a B.Sc. and M.Sc. degrees from Pontificia Universidad Católica de Chile and a PhD degree from Imperial College London, UK. He is currently an Assistant Professor at the University of Chile and a Research Associate at Imperial College. His research interests are power systems optimization, reliability and economics; renewable energy; and the smart grid.

Roberto Moreira (M'11) received his PhD from Imperial College London and is currently a Research Associate in this institution. His research interests include business models for energy storage and the various operational aspects like commercial strategies, degradation effects of battery storage, decentralized operation of distributed generation and multi-energy systems including heat networks.

Marcos Orchard received his B.S. degree and a Civil Industrial Engineering degree with Electrical Major from Catholic University of Chile. He also received his Ph.D. and M.S. degrees from The Georgia Institute of Technology, Atlanta, GA. He is currently an Associate Professor with the Department of Electrical Engineering at Universidad de Chile. His current research interest is the design, implementation and testing of real-time frameworks for fault diagnosis and failure prognosis, with applications to battery management systems, mining industry, and finance.

Goran Strbac (M'95) is a Professor of Energy Systems at Imperial College London. His current research is in modeling and optimization of economics and security of energy system operation and investment including integration of emerging technologies in supporting cost effective evolution to smart low carbon energy future.